# University of Groningen

## A Numerical Study on Wave Run up on an FPSO Bow

Buchner, B.; Bunnik, T.H.J.; Fekken, G.; Veldman, A.E.P.

Link to publication in University of Groningen/UMCG research database

# 01-1080

# A NUMERICAL STUDY ON WAVE RUN UP ON AN FPSO BOW

B. Buchner, MARIN

T.H.J. Bunnik, MARIN

G. Fekken, RuG

A.E.P. Veldman, RuG

## ABSTRACT

In this paper results are presented of numerical simulations of a wedge that penetrates the water surface. An extensive test series was carried out in which wedges were accelerated into the water with various velocities. These tests were done to study bow-flare slamming and the wave run up around the bow of an FPSO. Some of these tests were selected for the numerical simulations. The simulations have been carried with a Navier-Stokes solver based on a modified Volume Of Fluid (VOF) method that keeps track of the position of the free surface. The measured position of the wedge during the tests and the geometry of the wedge was put into the program to enable a reproduction of the tests. The simulations show the typical behavior of the water after the wedge has penetrated the water surface. Measured and calculated pressures are compared and show a good similarity. Measured and calculated wave elevations in front of the wedge are less similar due to the violent water behavior. The method is a promising tool for the analysis of wave-impact problems on realistic ship hulls.

## INTRODUCTION

Solid green water on the bow of Floating Production Storage and Offloading (FPSO) units in harsh environments is an important safety problem. This requires an optimum design of the hull shape. Based on model test data, in Ref [3] a new empirical method for the prediction of the strong non-linear relative wave motions around the bow has been presented. In Ref [4] this has been extended to the relation between the bow shape and the loading on structures at the deck.

In recent years, the University of Groningen has developed a numerical method, called COMFLO, that tracks the position of a free surface under various conditions. The method solves the Navier-Stokes equations with a free-surface condition on the boundary between fluid and air. Use is made of a modified Volume Of Fluid (VOF) algorithm. In first instance, the method was developed to deal with low-gravity waves and used to simulate the sloshing of liquid in satellites as described in Ref [5]. Results proved to be valuable and the tool so robust that since then spin-off has occurred in various other industrial applications. In Ref [6] the method was successfully applied to the sloshing of water inside anti-roll tanks. The method has already been applied to green-water problems. In Ref [7] results are shown of successful simulations of the flow of green water onto the deck of a non-moving FPSO.

In this paper, the method is applied to the rapid water entry of an accelerated wedge. Previous work by Arai and Matsunaga, see Ref [2] and Arai and Tasaki, see Ref [1] showed that the VOF algorithm was capable of predicting the free-surface flow and pressure loads on a wedge after rapid water entry. However, in their method the wedge was fixed in space and water flows in with constant speed from the bottom of the domain. In the present method, the wedge may move relative to the grid with any prescribed motion. Therefore, it is possible to simulate experiments very accurately.

At MARIN, model tests have been carried out with a two-dimensional accelerated wedge with a flare angle of 30 degrees. During these tests, a pressure transducer measured the pressure load on the wedge and the wave run up was measured in front of the wedge. Two tests have been selected for this study. The time traces of the position of the wedge during the tests have been used as input to the program. The pressure on the wedge and the relative wave height in front of the wedge are compared with the output from the numerical simulation.

## NOMENCLATURE

- $\vec{u}$      : velocity of fluid particle [ $\mathrm{ms}^{-1}$ ]
- $u_n$      : normal velocity of fluid particle [ $\mathrm{ms}^{-1}$ ]
- $u_t$      : tangential velocity of fluid particle [ $\mathrm{ms}^{-1}$ ]

- $\nabla$          : gradient operator $[\,\mathrm{m}^{-1}\,]$
- t           : time $[\,\mathrm{s}\,]$
- $\sigma$         : surface tension $[\,\mathrm{Nm}^{-1}\,]$
- $\kappa$         : surface curvature $[\,\mathrm{m}^{-1}\,]$
- $\rho$         : density $[\,\mathrm{kgm}^{-3}\,]$
- p          : pressure $[\,\mathrm{Nm}^{-2}\,]$
- $\Delta$         : Laplace operator $[\,\mathrm{m}^{-2}\,]$
- $\nu$         : kinematic viscosity $[\,\mathrm{m}^{2}\mathrm{s}^{-1}\,]$
- $\tau$         : tangential stress $[\,\mathrm{s}^{-1}\,]$
- g          : gravitational acceleration $[\,\mathrm{ms}^{-2}\,]$
- $\vec{e}_3$        : unit vector pointing upwards [-]

## MATHEMATICAL AND NUMERICAL DESCRIPTION OF THE METHOD

The Navier-Stokes equations describe the motions of a fluid in general terms. They are based on conservation of mass and momentum:

$$\nabla \cdot \vec{u} = 0$$

$$\frac{\partial \vec{u}}{\partial t} + \left(\vec{u} \cdot \nabla\right)\vec{u} = -\frac{\nabla p}{\rho} + \nu\Delta\vec{u} - g\vec{e}_3$$

The numerical tool solves these Navier-Stokes equations in complex three-dimensional geometries. Free-surface effects are modeled as well. Moving objects have been implemented the program. Until now, the geometries are restricted to 2D-shapes. On the boundaries of the fluid domain boundary conditions have to be prescribed. Several options are possible:

1.  On a solid boundary, either the no slip condition
$$\vec{u} = \vec{0}$$
is used, or the free slip conditions
$$\vec{u} \cdot \vec{n} = 0, \qquad \tau = \frac{\partial u_t}{\partial n} = 0$$

2.  On an inflow boundary, the velocity is prescribed

3.  On an outflow boundary, the pressure is prescribed and for the velocity a homogeneous Neumann condition is used
$$\frac{\partial \vec{u}}{\partial n} = 0$$

4.  On the free surface boundaries, the dynamic conditions hold to ensure that the free-surface pressure equals the atmospheric pressure and to ensure that the air does not exert tangential forces on the free surface. This is described
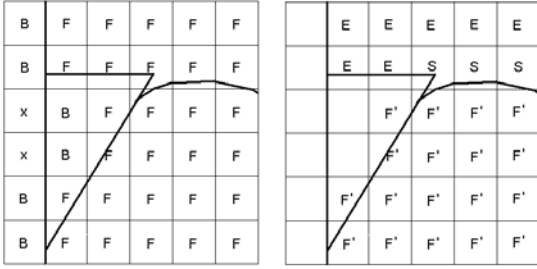
by $$\frac{p - p_0}{\rho} = \nu\frac{\partial \vec{u}_n}{\partial n} - \frac{\sigma\kappa}{\rho},$$

$$\nu\left(\frac{\partial u_n}{\partial t} + \frac{\partial u_t}{\partial n}\right) = 0$$

In the simulations shown in this paper, only the no-slip condition and the dynamic free-surface conditions are used. In the latter, the term $\nu\dfrac{\partial \vec{u}_n}{\partial n}$ is neglected.

The fluid domain is discretized with a Cartesian grid, not necessarily equidistant. An indicator function is used in the form of so-called volume and edge apertures to track the amount of flow in a cell and through a cell face:

- Volume aperture - The geometry aperture $F_b$ indicates which fraction of a cell is allowed to contain fluid ($0 \le F_b \le 1$). For bodies moving through the fluid, the geometry aperture may vary in time. The time-dependent fluid aperture $F_s$ indicates which fraction of a cell is actually occupied by fluid and satisfies the relation $0 \le F_s \le F_b$.
- Edge aperture - The edge apertures $A_x$, $A_y$, and $A_z$ define the fraction of a cell surface through which fluid may flow. Obviously these apertures are between zero and one.

After the apertures have been assigned to the grid cells and the cell edges, every cell is given a label to distinguish between boundary, air and fluid. Two classes of labeling exist: Geometry cell labels and fluid cell labels. The geometry labeling at each time step divides the cells in three classes:

- **F**(luid)-cells         : All cells with $F_b \ge 0$
- **B**(oundary)-cells      : All cells adjacent to a **F**-cell
- (e)**X**(ternal)-cells      : All remaining cells

The fluid cell labeling is a subdivision of the **F**-cells. The subdivision consists of 3 subclasses:

- **E**(mpty) cells          : All cells with $F_s = 0$
- **S**(urface) cells        : All cells adjacent to an **E**-cell
- **F'**-cells            : All remaining **F**-cells

**Figure 1: Geometry cell labeling (left) and free-surface cell labeling (right) for a wedge entering a fluid**
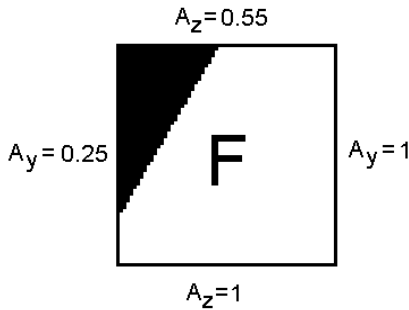


**Figure 2: Edge apertures for a grid cell containing part of the wedge**

The discretisation of the Navier-Stokes equations is done on a staggered grid, so pressures are set in cell centers and velocities in the middle of cell faces. The Navier-Stokes equations are discretized in time as follows:

$$\nabla \vec{u}^{n+1} = 0$$

$$\frac{\vec{u}^{n+1} - \vec{u}^n}{\Delta t} + \nabla p^{n+1} = \vec{R}^n$$

where $\Delta t$ is the time step and n+1 and n denote the new and old time level. $\vec{R}^n$ contains all convective, diffusive and body forces. These two equations can be combined into a Poisson equation for the pressure. The time step is variable and is chosen such that the fluid is transported over no more than one cell in one time step.

The discretisation in space is more complicated and depends on the kind of cells between which a cell face is positioned. A more detailed description of the space discretisation for solid fixed boundaries can be found in Refs [5-7].Moving objects still create some complications, as will be discussed below.

After discretisation and insertion of the boundary conditions, the velocities and pressures at the new time level are determined. After calculating the flux through cell faces, the new fluid apertures $F_s$ and the new cell labeling can be determined.
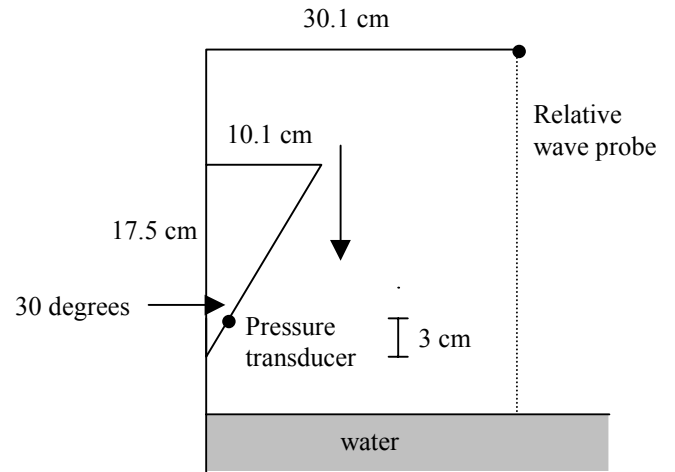
**TEST SET UP**



**Figure 3: The test set up**

Figure 3 shows the test set up for the wedge with a flare angle of 30 degrees. On the edge of the wedge, a pressure transducer has been placed that measures the pressure impact of the wedge when it penetrates into the water. 20 centimeters in front of the wedge, the relative wave height is measured. The wave height can be obtained by subtracting the motion from the relative wave height. In all figures that show the relative wave height, the motion is therefore shown as well.

**NUMERICAL SET UP**

A large number of experiments with wedges of 30 degrees-flare angle has been carried out by MARIN. From these measurements, 2 were selected and reproduced as accurately as possible by the method:

1) A wedge with 30-degrees flare angle, starting 20 cm above the water surface, that is entirely submerged and not lifted out of the water. The mean velocity of the wedge is 1.43 m/s.
2) A wedge with 30-degrees flare angle, starting on the water surface, that is not entirely submerged and lifted out of the water. The mean velocity is 0.54 m/s.

In this paper, we will refer to these tests as test cases 1 and 2.

Measurements were also done for a wedge that got entirely submerged and was lifted out of the water again. These could not be reproduced accurately because equipment was placed on top of the wedge during the measurements, obstructing the water flow.

The following figure shows the computational domain and the coordinate system at the start of the simulation for the wedge with a 30-degree flare angle. The gray area contains water. In this figure, the wedge is shown to start on the waterline. The water depth is one meter and the horizontal size of the domain is 1 meter to keep the number of grid cells and computational time relatively small. A total of 50 cells was used in vertical direction and 50 in horizontal direction.
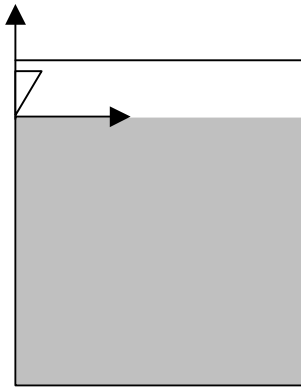


**Figure 4: Computational domain for the numericak simulations**

As mentioned, configurations with wedges starting 20 cm above the water surface were simulated as well. In these tests, the entrance velocity was significantly larger, which creates a more violent water flow.

During the tests, the position of the wedge was measured. This position and the corresponding velocity of the wedge served as input for the numerical tool. Because the measured position contains high-frequency noise, it was first filtered to enable accurate numerical differentiation. This results in the curves in the following 2 figures:
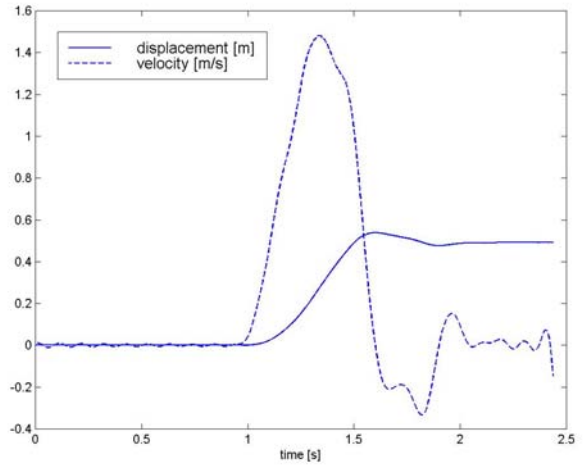


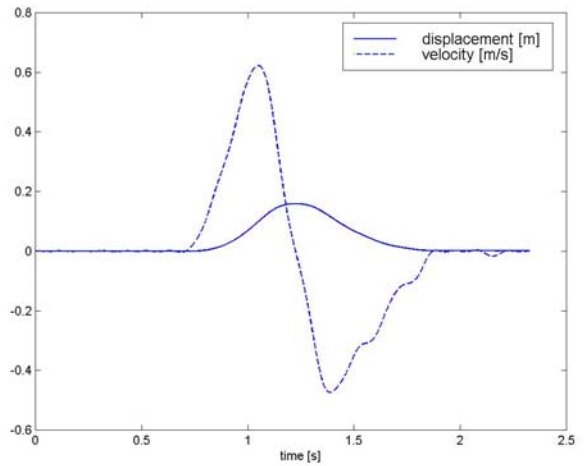**Figure 5: Vertical displacement and velocity of the wedge in test case 1.**



**Figure 6: Vertical displacement and velocity of the wedge in test case 2.**

## RESULTS

During the simulations, the pressure was measured on the wedge and the relative wave elevation in front of the wedge. The relative wave height was measured 20 cm in front of the wedge.

The simulations show that the pressure contains inaccuracies, especially directly after the high-velocity water entry. A reason for this behavior is the change in free-surface labels, which occurs when the water surface moves along the wedge. In combination with solid walls cutting diagonally through the grid, this free-surface label change induces a clearly visible spike in the pressure. A similar situation still occurs when a geometry label changes, due to the motion of the solid body.

This behavior is shown in the next figure where the measured pressure is compared with the computed pressure as it comes out of the numerical tool.
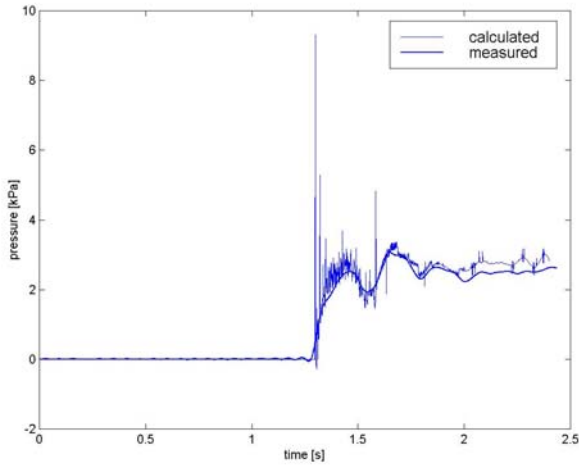


**Figure 7: Measured and unfiltered calculated pressure for test case 1.**

However, when the computed signal is filtered and the high-frequency oscillations are removed, the agreement between measurement and calculation is good. This is shown in the next figure. Therefore, in the remainder of this paper, only the filtered signals are shown. In future research, the problem of the spikes in the pressure signal needs further investigation. This figure also shows that, due to the high velocity of the wedge, the pressure differs significantly from the hydrostatic pressure.
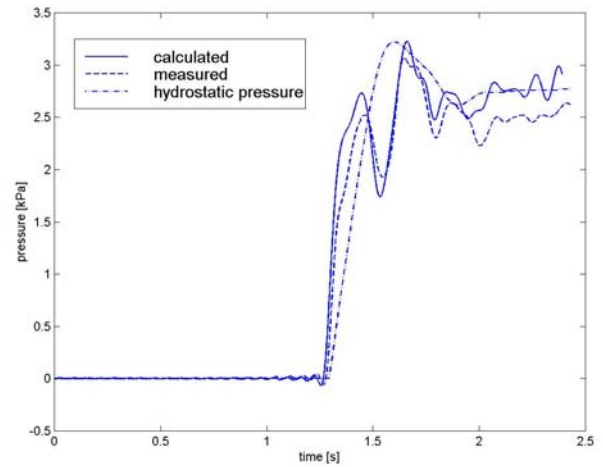
The calculated relative wave height in front of the wedge shows the same behavior as the measured one. However, the initial high-velocity wave tongue is underestimated. It is likely that this is related to the same problems as for the pressure impact.

In test case 2, the entrance velocity of the wedge is much smaller and the water reaction less violent. Therefore, the pressures are more in line with the hydrostatic pressure. The peak pressure is less than for the previous simulation because the wedge is not entirely submerged.

The relative wave elevation in front of the wedge is better predicted than in the previous simulation. The initial wave elevation is predicted correctly now. The remainder of the wave signal looks very similar to the test results although there is a small shift in the wave pattern after 1.5 seconds.
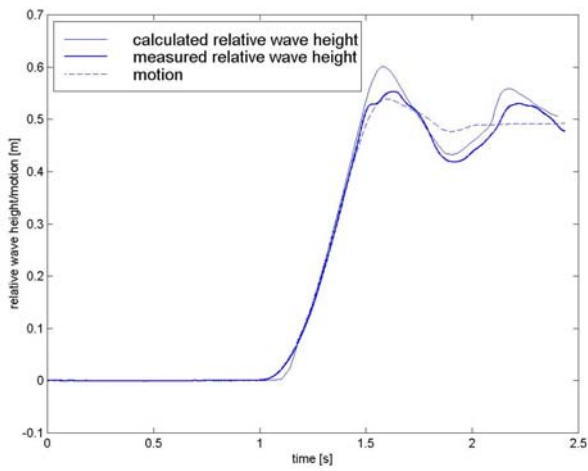


**Figure 8: Measured and filtered calculated pressure for test case 1.**

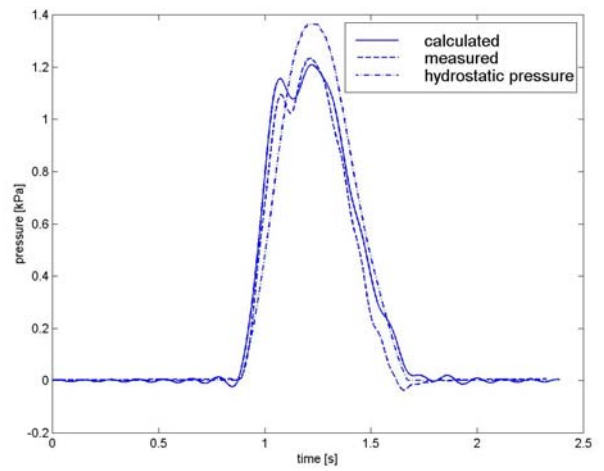**Figure 9: Measured and calculated relative wave height for test case 1.**



**Figure 10: Measured and filtered calculated pressure for test case 2.**

modifications are made to the method that will solve this problem.

The results of this study indicate that the method is capable of predicting pressure loads on moving geometries in 2 dimensions. The principle is the same in three dimensions, although the implementation is far more difficult than in two dimensions. It is expected that in a few years the method will be sufficiently extended and improved to give a reliable prediction of pressure loads on realistic ship hulls.

## REFERENCES

[1] Arai, M. and Tasaki, R., "A numerical study of Water Entrance of Two-dimensional wedges --- Effect of Gravity, Spray Generation and vertical load", PRADS, June 1987, Trondheim.

[2] Arai, M. and Matsunaga, K., "A numerical study of Water Entry of Two-dimensional ship-shaped bodies", PRADS, 1989.

[3] Buchner, B., "A new method for the prediction of Non-Linear Relative Wave Motions", OMAE98, June 1998, Lisbon.

[4] Buchner, B. and Voogt, A., "The Effect of Bow Flare Angle on FPSO Green Water Loading", OMAE2000, February 2000, New Orleans.

[5] Gerrits, J., Loots, G.E., Fekken, G. and Veldman, A.E.P., "Liquid sloshing on earth and in space", In: Moving boundaries V (B. Sarler, C.A. Brebbia and H. Power eds) WIT Press, Southampton 1999, pp. 111-120.

[6] van Daalen, E., Kleefsman, K., Gerrits, J., Luth, H.R., Veldman, A.E.P., "Anti Roll Tank Simulations with a Volume of Fluid (VOF) based Navier-Stokes Solver", 23rd Symposium on Naval Hydrodynamics, September 2000, Val de Reuil.

[7] Fekken, G., Veldman, A.E.P. and Buchner, B., "Simulation of green water loading using the Navier-Stokes equations", NSH7, July 1999, Nantes.
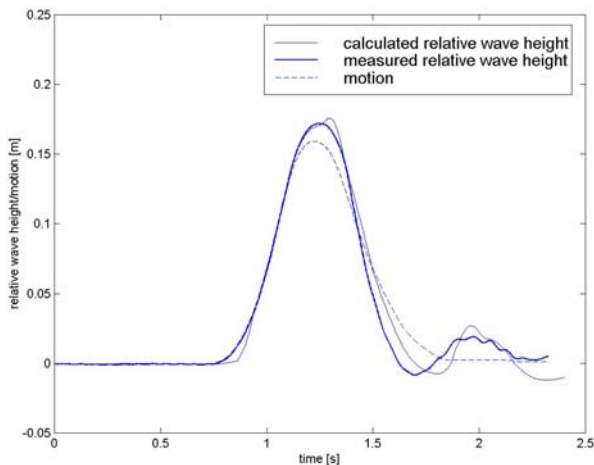
**Figure 11: Measured and calculated relative wave height for test case 2**

## CONCLUSIONS

The numerical tool was successfully used to simulate the water penetration of a wedge with a flare angle of 30 degrees. An accurate simulation of similar model tests was possible by putting the time traces from the measurements and the wedge geometry directly into the program. A high and low-velocity water entry was simulated which showed that the typical behavior of the water right after the entry of the wedge could be reproduced. The pressure loads on the wedge were compared and even for the high-velocity water entrance the calculation comes very close to the measurement. There is however still a problem with the combination of free-surface motion and diagonal geometries in a Cartesian grid that causes numerical inaccuracies in the pressure iteration. At the moment